Wealth Thermalization Hypothesis

Klaus M. Frahm[1] and Dima L. Shepelyansky[1]

[1]*Laboratoire de Physique Théorique, Université de Toulouse, CNRS, UPS, 31062 Toulouse, France*

(Dated: June 19, 2025; Revised: XXXX)

We introduce the wealth thermalization hypothesis according to which the wealth shared in a country or the whole world is described by the Rayleigh-Jeans thermal distribution with two conserved quantities of system wealth and norm or number of agents. This distribution depends on a dimensional parameter being the ratio of system total wealth and its dispersion range determined by highest revenues. At relatively small values of this ratio there is a formation of the Rayleigh-Jeans condensate, well studied in such physical systems as multimode optical fibers. This leads to a huge fraction of poor households and a small oligarchic fraction which monopolizes a dominant fraction of total wealth thus generating a strong inequality in human society. We show that this thermalization gives a good description of real data of Lorenz curves of US, UK, the whole world and capitalization of S&P500 companies at New York Stock Exchange. Possible actions for inequality reduction are briefly discussed.

PACS numbers:

Introduction. The wealth distribution in the human society is characterized by a striking inequality (see e.g. [1–3]). Thus for the whole world 50% of the population owns only 2% of total wealth, while 10% of population owns 75% of total wealth and 1% of population owns 38% of total wealth [2].

The distribution of wealth is usually described by the Lorenz curve [3, 4] which gives the dependence of cumulated normalized wealth $0 \leq w \leq 1$ on the cumulated normalized fraction of population or households $0 \leq h \leq 1$. Thus the equipartition of wealth corresponds to the diagonal $w = h$ and the doubled area between diagonal and the Lorenz curve $w(h)$ determines the Gini coefficient $0 \leq G \leq 1$ [3, 5]. Values of G can be found in [6] for world countries in 2021 being in the range $0.59 < G < 0.90$; for the whole world $G = 0.889$.

The sharing of wealth varies from country to country but the global features remain rather similar with a big fraction of very poor population with scanty wealth and a very small fraction of rich people having a significant fraction of a country's total wealth. This gives an insight that some fundamental underground reasons can be at the origin of this inequality.

Diverse methods of statistical mechanics and physical kinetics [7–9] have been proposed and used by different research groups [10–18]. Various models of interacting agents are investigated including Random Asset Exchange models [10–18]. In several of these models there is appearance of some kind of oligarchic phase with a significant wealth accumulation by a group of agents [13, 16–18]. The specific arguments are presented in a favor of the Boltzmann-Gibbs type description of distribution of money, wealth and income [12, 14]. Also a nonlinear Fokker–Planck description of asset exchange is proposed [16, 17] with emergence of oligarchic phase. A few important elements are stressed in [16, 17]: the conservation of two integrals of system evolution being the total wealth and total norm (or number of agents), the argument in favor of consideration of wealth instead of money based on the small-transaction approximation.

The above models give interesting insights for understanding of certain features of wealth distribution in the world countries but they remain model specific and their universality remains questionable. The universality of the Boltzmann-Gibbs thermal distribution is the ground element of the approach developed in [12, 14] but it does not capture emergence of a huge condensate of poverty in various countries.

Our studies here are based on the Wealth Thermalization Hypothesis (WTH) according to which the wealth of a country is described by the Rayleigh-Jeans (RJ) thermal distribution:

$$\rho_m = \frac{T}{E_m - \mu} \ \text{(RJ)}. \tag{1}$$

Here we assume that the system wealth has certain states $0 \leq m < N$ with energies E_m and the population probabilities in these states are ρ_m. Also T is the system temperature and $\mu(T)$ is the chemical potential dependent on T. As in [16] there are two conserved integrals of motion being the total norm of population, fixed to be unity for convenience, $\sum_m \rho_m = 1$, and the system average wealth being its total energy $\sum_m E_m \rho_m = E$. For a given system energy E and unity norm these two integrals of motion determine the system temperature T and its chemical potential $\mu(T)$. The entropy S of the system is determined by the usual relation [7, 8]: $S = -\sum_m \rho_m \ln \rho_m$ with the implicit theoretical dependencies on temperature $E(T)$, $S(T)$, $\mu(T)$.

The RJ thermalization (1) is universal and describes a variety of classical systems [7, 8] including nonlinear waves [19], light propagation in multimode optical fibers with a nonlinear media [20–24], dynamical thermalization for nonlinear perturbation of the Random Matrix

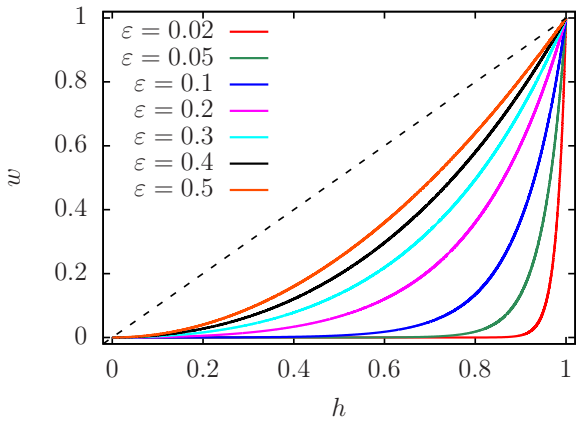

FIG. 1: Lorenz curves for the RJS model with the linear spectrum $E_m = m/N$ (for $N = 10000$) for different values of the rescaled energy $\varepsilon = E/B$. The x-axis corresponds the cumulated fraction of households (h) and the y-axis to the cumulated fraction of wealth (w). The dashed line is the line of perfect equipartition $w = h$. The Gini coefficients G for all curves are $G = 0.9600, 0.9000, 0.8006, 0.6250, 0.4990, 0.4066, 0.3333$ (bottom to top).

Theory (RMT) [25] and the nonlinear Schrödinger equation (NSE) in quantum chaos billiards [26]. It is pointed out in [27–29] that RMT finds a variety of applications in multiple areas of physics including nuclei, complex atoms and systems of quantum chaos whose dynamics is chaotic in the classical limit. Thus almost any physical nonlinear interaction above a chaos border [25] leads to dynamical RJ thermalization (1). An example of such a system can be an ensemble of N nonlinear RMT oscillators with random frequencies $\omega_m \propto E_m$ of an ensemble of N agents with nonlinear interactions leading to the RJ thermalization (1). The thermalization can have a dynamical origin when chaotic nonlinear dynamics leads to (1) or it can appear due to an external thermal bath. We suppose that for WTH a dynamical origin is more adequate since in a first approximation on a scale of one year a country or the whole world can be considered to be quasi-isolated from slow external processes.

Due to the presence of two integrals of motion, energy and norm, RJ thermalization has the phase of RJ condensate emerging at relatively low total energy E or low temperature T [20, 21, 26]. Thus at low energy and a big number of oscillators, as in [25], or a big number of interacting agents, the fraction of RJ condensate is approaching unity being concentrated at a vicinity of the ground state energy E_0 being zero or very close to zero [26]. Thus the RJ condensate (1) very naturally has a huge fraction of very poor agents that naturally describes the huge world wealth inequality where 50% of population owns only 2% of the total wealth [2]. Below we describe in detail various consequences of WTH (1) and compare the results of this theory with real Lorenz curves of certain countries and the whole world.

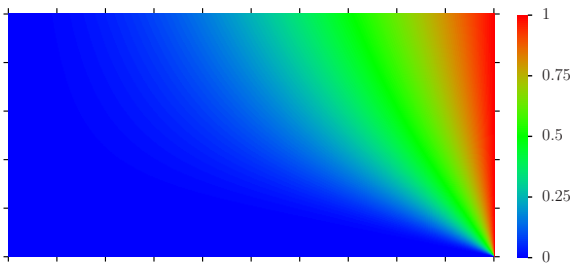

FIG. 2: Color plot of wealth w from Lorenz curves of the RJS model ($N = 10000$). The x-axis corresponds to the fraction of households $h \in [0, 1]$ and the y-axis to the rescaled energy $\varepsilon = E/B \in [0, 0.5]$. The ticks mark integer multiples of 0.1 for h and ε.

RJ thermalization and condensation. We start from a model with N equidistant energy levels $0 \leq E_m = m/N \leq B$ located in the energy band of total width B. This corresponds to certain levels of wealth for N agents with a fraction of agents on level m being ρ_m. The conserved average system energy is $E = \sum_m E_m \rho_m$ and the dimensionless parameter $\varepsilon = E/B$ determines its fraction with respect to the maximal system energy B. We call this model the RJ standard (RJS) model. On the basis of WTH with RJ distribution (1) the local (normalized) wealth on level i is $(E_i/E)\rho_i$ and the cumulated wealth on levels $[0, m]$ is $w = \sum_{i=0}^{m} (E_i/E)\rho_i$ with the cumulated fraction of population or households $h = \sum_{i=0}^{m} \rho_i$. Computing both sums for all values of $m = 0, 1, \ldots$ provides the Lorenz curve $w(h)$. Since the Lorenz curve describes the normalized distribution of cumulated fractions of wealth $w \in [0, 1]$ and households $h \in [0, 1]$ we use the ratio E_i/E (since $E = \sum_i E_i \rho_i$) in the definition of wealth ensuring that $w = 1$ at $h = 1$ for the total population. At given ε the relation (1) and two integrals of energy and norm determine the physical parameters T, μ, S. In our numerical studies we use $N = 10000$ which practically corresponds to the continuous limit with results independent of N. The dependencies of T and μ on ε in the RJS model are shown in Supplementary Material (SupMat) Fig. S1. As discussed in [25, 26] for $\varepsilon > 1/2$ the temperature T becomes negative and at ε close to unity there is a formation of an RJ condensate on highest energy levels with $E_m \to B$ (see SupMat Fig. S2). Many unusual properties of RJ thermalization have been discussed in [25, 26] but for convenience we provide some details in SupMat and Figs. S2 and S3 show the dependence of ρ_m on E_m/B for certain values of ε with a clear formation of an RJ condensate at small ε or $1-\varepsilon$. Even if the regime with negative temperatures has been realized in fiber experiments [24] we consider that such a regime is not applicable to human society and hence we consider only the range with $0 \leq \varepsilon \leq 1/2$.

The Lorenz curves for the RJS model at several ε val-

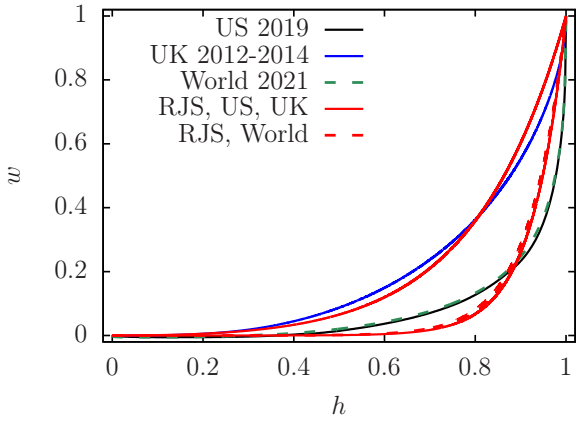

FIG. 3: Comparison of the Lorenz curves for US 2019 (black), UK 2012-2014 (blue), World 2021 (dashed green) with those of RJS model (red curves; $N = 10000$); US and World curves are rather close. For the three referenced curves Gini coefficients are $G = 0.852$, 0.626, $G = 0.842$ respectively and the rescaled energies $\varepsilon = E/B$ of RJS model are respectively fixed as $\varepsilon = 0.07420$, $\varepsilon = 0.1996$, $\varepsilon = 0.07911$ so that the corresponding Gini coefficients match the referenced data.

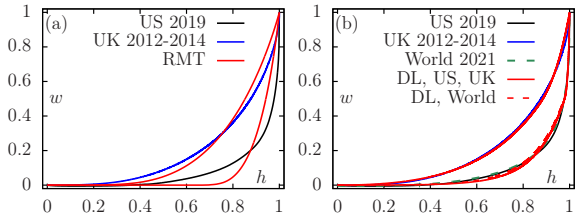

FIG. 4: Both panels compare the Lorenz curves for different data sets (black for US 2019, blue for UK 2012-2014 and green dashed for World 2021) with those of the RMT model (a) and the DL model (b). As in Fig. 3 the Gini coefficients G of the reference curves are used to fix the rescaled energy $\varepsilon = E/B$ of the corresponding model such that the model curves (red) have the same G. For the RMT model (a) only two data sets are shown $\varepsilon = 0.07996$ (US) and $\varepsilon = 0.2027$ (UK). For the DL model (b) the parameter values are $a = 16$ (US and World) and $a = 3$ (UK). These values are fixed to have a best possible fit of the model data with those of the reference curves. The chosen values $\varepsilon = 0.01434$ (US), $\varepsilon = 0.1355$ (UK), $\varepsilon = 0.01535$ (World) match the G values of the reference data. In (b) the curves for US and World are rather close and a zoomed view is given in SupMat Fig. S4. In (a) the RMT Lorenz curves are shown for one realization of a random matrix, other realizations give practically the same curves.

ues are shown in Fig. 1. Due to RJ condensate there is a very high fraction of poor households f_p (with $w \leq 0.02$) and a small fraction of rich ones f_r (with $w \geq 0.75$) who owns a huge fraction of total wealth. Thus the RJS model naturally describes the big phase of poor households and the oligarchic phase of small fraction of households capturing the big fraction of total wealth. At maximal $\varepsilon = 0.5$ with $(\mu \to -\infty)$ all ρ_m are equal and hence the Lorenz curve is $w = h^2$ with the limiting minimal Gini coefficient $G = 1/3$ for the RJS model. The dependence of cumulated wealth w on h and ε is shown in Fig. 2. It clearly shows the phase of poor households (blue), corresponding to the RJ condensate, and the oligarchic phase of very rich households (red). Thus we see that the RJ thermal distribution (1) describes the main qualitative features of wealth inequality of human society [2].

From Figs. 1, 2 we see that for the RJS model the WTH based on (1) captures main elements of wealth inequality but it is important to see if it can reproduce the real Lorenz curves for the whole world and specific countries. For this comparison of WTH theory we choose three cases with the Lorenz curves for: the whole world from [2] (integration of front page data gives cumulative w, h values); USA 2019 case from [30] and UK 2012-2014 case from [31]. These real Lorenz curves are compared with those obtained from the RJS model (1) in Fig. 3. For the comparison values of ε are fixed in such a way that Gini coefficient is the same for theory and real data curves. The comparison for UK case shows that there is a good agreement of real and theoretical Lorenz curves even if there is a certain difference for the range $0.9 \leq h \leq 1$. The difference is more visible for USA case and the whole world (Lorenz curves are very similar for these two cases). In SupMat Fig. S4, we also show that the the RJS Lorenz curves have a satisfactory agreement with the Lorenz curves for France and Germany (data are obtained for the year 2010 from [32]).

In view of certain differences between real Lorenz curves and those obtained from RJS model (see Fig. 3) we also study the case of RJ distribution (1) with level energies E_m taken from a random matrix of size $N = 1000$ as it was discussed in [25]. For this RJ RMT model the density of states is $\nu = dm/dE_m = \frac{2N}{\pi}\sqrt{1 - E^2}$ with typical eigenvalues in the interval $E_m \in [-1, 1]$ and we shift all E_m to $E_m - E_0$ to have nonnegative values $E_m \geq 0$ in (1). The comparison of Lorenz curves for US and UK cases with the results of the RJ RMT model is shown in Fig. 4a. The similarity between real and RMT model data is a bit less good then those in Fig. 3 for the RJS model. This shows that the density of states ν can affect the Lorenz curves. Indeed, we have $\nu = $ const. for the RJS model being different from the semi-circle law of RMT model.

To reproduce the real Lorentz curves from [2, 30, 31] in a better way we also analyze a double-linear (DL) model with energies $E_m = m/N$ for $m < N/2$ and $E_m = E_{N/2} + a(m - N/2)/N$ for $m \geq N/2$ at $N = 10000$ with $a = 16$ $(B = 8.5)$ for US and World data, and $a = 3$ $(B = 2)$ for UK data. In this type of model the density of states takes not one but two values being $\nu = 1$ and $\nu = 1/a$. The existence of two ν values can correspond to a society where high wealth energy E_m values are only accessible to very rich people whose density is lower compared to

common people. The comparison of real Lorenz curves with those of the DL model is shown in Fig. 4b (and its zoomed version SupMat Fig. S5) demonstrating a better proximity between real Lorenz curves and those from the DL model as compared to the results of the RJS model in Fig. 3. However, the DL model has two fit parameters a, ε while the RJS model has only one ε.

We also remind that for the RJS model the minimal Gini value is $G = 1/3$ that is reached at maximal physical value of $\varepsilon = 1/2$. Thus to have $G < 1/3$, we need to significantly modify the density of states ν. Indeed, we can obtain a perfect complete wealth and energy equipartition with $w = h$ and $G = 0$ for the case when all $E_m = E_0$ values are the same. In this case, the integrals of energy and norm give only one conservation law and all states have the same energy and same population. A small spectrum modification to $E_m = E_0 + m/N$ with a constant energy offset E_0 leads to Lorenz curves being closer to the diagonal with small Gini values $G < 1/3$ and a finite slope $w(h) \approx [E_0/(\varepsilon + E_0)]\, h$ at small h (see SupMat with additional discussion of this model and related Fig. S6). We call this model the equipartition (EQI) model.

We also show color Figures analogous to Fig. 2 for various models discussed above (see SupMat Fig. S7). We note that assuming the validity of RJ distribution (1) it is possible to try to extract the spectrum E_m from the real Lorenz curve data by an inverse operation. However, we find that this inversion procedure is very sensitive to the exact curve shape $w(h)$ (quality of raw data), also additional fit parameters should be added (and not only two as in the above DL model), so that we do not go in more details here with this approach.

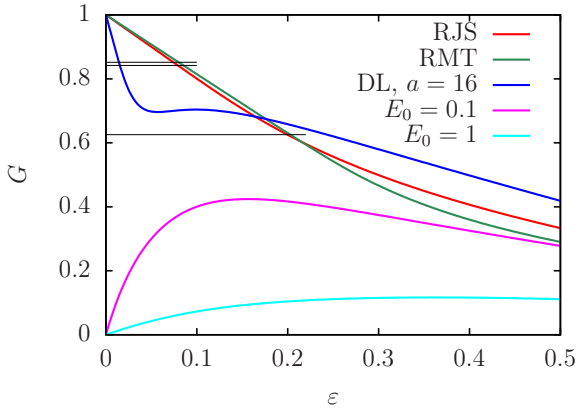

FIG. 5: Gini coefficient versus rescaled energy $\varepsilon = (E - E_0)/(E_{N-1} - E_0)$ for the RJS model (red), RMT model (green), DL model (blue; only for the case $a = 16$), and the EQI model (pink for the offset $E_0 = 0.1$ and cyan for $E_0 = 1$; same values of E_0 are used in SupMat Fig. S6). The thin black lines show the values of $G = 0.852$, $G = 0.842$ and 0.626 for the data of US 2019, World 2021 and UK 2014. The intersection of these lines with the red and green curves correspond to ε values used in Figs. 3, 4.

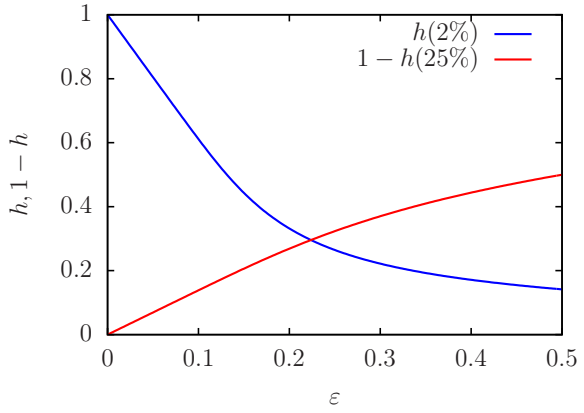

FIG. 6: Dependence of fraction of poor households $f_p = h(2\%)$ (owning 2% of wealth) and fraction of rich oligarchic households $f_r = 1 - h(25\%)$ (owning 75% of wealth) on the rescaled energy $\varepsilon = E/B$ for the RJS model.

The dependence of the Gini coefficient G on ε is given in Fig. 5 for the different models. In global the results show that an increase of ϵ leads to a reduction of G. Also in Fig. 6, we show the dependence of fractions of poor f_p and rich oligarchic f_r households on ε for the RJS model. Thus at $\varepsilon = 0.07$ we have $f_p = 0.73$ and $f_r = 0.097$ that is close to the real values $f_p = 0.53$(US), 0.5(World) and $f_r = 0.09$(US), 0.1 (World) while for UK we have $f_p = 0.32$, $f_r = 0.28$ corresponding to a higher $\varepsilon \approx 0.21$. Furthermore Fig. 6 shows that the fraction of poor households can be significantly reduced and the fraction of rich households can be increased by increasing parameter ε, thus diluting the oligarchic phase.

Finally, we mention that for the RJS model it is possible to work out analytic expressions (at $N \to \infty$; see SupMat section III) for the Lorenz curve and other quantities that accurately match the numerical data (see SupMat Fig. S8). These expressions depend on μ and at small $\varepsilon \leq 0.2$ (with $\mu \approx 0$), we have $w(h) \approx e^{(h-1)/\varepsilon}$ and $G \approx 1 - 2\varepsilon$, matching 3 values of G in Fig. 1.

Discussion. In this work, we use the WTH approach (1 to describe the wealth distribution in a closed system that may be a country or the whole world. Our main argument is that in such a system interaction of agents is described by nonlinear equations with the conservation of two integrals of motion being total number of agents (norm or total probability analogous to number of system particles) and total wealth (analogous to total system energy). Under these conditions the wealth sharing is described by the universal RJ thermal distribution (1) as it is the case for various physical systems [7, 8, 19–26]. The striking feature of RJ thermalization (1) is that at low system energy (low ε) there is the physical phenomenon of RJ condensation when a high fraction of total probability is located at lowest energy states that corresponds to the high fraction of poor households with very low wealth and also other small fraction of oli-

garchic households that monopolize a big fraction of total wealth. Thus according to the WTH the phenomenon of huge wealth inequality in the world [1, 2] finds a natural thermodynamic explication. We show that the WTH theory gives a good description of the Lorenz curves of US, UK and the whole world.

On the basis of WTH theory we see that a reduction of wealth inequality can be realized by an increase of rescaled system energy ($\varepsilon = e/B$). The simplest way to reach this is to reduce the global dispersion of wealth (given by B) that can be realized by a high taxation of high wealth revenues.

Universality of WTH theory is also confirmed by showing that it well describes the Lorenz curves of capitalization of companies at S&P500 of New York Stock Exchange (NYSE), London SE, Hong Kong SE (see SupMat Figs. S9, S10, S11,S12 with data from [33–35]).

Acknowledgments: This work has been partially supported through the grant NANOX N^o ANR-17-EURE-0009 in the framework of the Programme Investissements d'Avenir (project MTDINA).

[1] T. Piketty, *Capital in the Twenty-First Century*, Belknap Press of Harvard University Press, Cambridge, MA (2014).

[2] L. Chancel, T. Piketty, E. Saez, G. Zucman *et al. World Inequality Report 2022*, World Inequality Lab `https://wir2022.wid.world` (Accessed on 8 June 2025).

[3] B. Roach, P. J. Rajkanikar, N. Goodwin, and J.Harris, *Social and Economic Inequality*, An ECI Teaching Module on Social and Environmental Issues, Economics in Context Initiative, Global Development Policy Center, Boston University (2023), `https://www.bu.edu/eci/files/2023/05/Inequality-Module-2023.pdf` (Accessed 8 June 2025).

[4] M.O. Lorenz, *Methods of measuring the concentration of wealth*, Quarterly Publications of the American Statistical Association, **9**, (New Series, No. 70), 209–219 (1905); `https://doi.org/10.1080/15225437.1905.10503443` (Accessed 8 June 2025).

[5] C. Gini, *Sulla misura della concentrazione e della variabilit'a dei caratteri*, Atti del Reale Istituto Veneto di Scienze, Lettere ed Arti, **73**, 1203–1248 (1914); English translation in Metron - Int. J. Statisrics, **63**, 3–38 (2005); `https://www.dss.uniroma1.it/RePec/mtn/articoli/2005-1-1.pdf` (Accessed 8 June 2025).

[6] Wikipedia, *List of sovereign states by wealth inequality*, `https://en.wikipedia.org/wiki/List_of_sovereign_states_by_wealth_inequality` (Accessed 8 June 2025).

[7] J.E. Mayer, M. Goeppert-Mayer, *Statistical mechanics*, John Wiley & Sons, N.Y. (1977).

[8] L.D. Landau, and E.M. Lifshitz, *Statistical physics*, Wiley, New York (1976).

[9] E.M. Lifshitz and L.P. Pitaevskii, *Physical kinetics*, Pergamon Press N.Y. (1995).

[10] J. Angle, *The surplus theory of social stratification and the size distribution of personal Wealth*, Soc. Forces **65**, 293 (1986).

[11] S. Ispolatov, P. L. Krapivsky, and S. Redner, *Wealth distributions in asset exchange models*, Eur. Phys. J. B. **2**, 267 (1998).

[12] A. Dragulescu, and V. Yakovenko, *Statistical mechanics of money*, Eur. Phys. J. B. **17**, 723 (2000).

[13] J.-P. Bouchaud, and M. Mezard, *Wealth condensation in a simple model of economy*, Physica A **282**, 536 (2000).

[14] V. M. Yakovenko, and J. B. Rosser, *Colloquium: Statistical mechanics of money, wealth, and income*, Rev. Mod. Phys. **81**, 1703 (2009).

[15] B. K. Chakrabarti, A. Chakraborti, S.R. Chakravarty, and A. Chatterjee, *Econophysics of income and wealth distributions*, Cambridge University Press, N.Y. (2013).

[16] B. M. Boghosian, A. Devitt-Lee, M. Johnson, J. Li, J. A. Marcq, and H. Wang, *Oligarchy as a phase transition: the effect of wealth-attained advantage in a Fokker–Planck description of asset exchange*, Physica A **476**, 15 (2017).

[17] B. M. Boghosian, *The inescapable casino*, Sci. American, November, 71 (2019).

[18] N. V. Von Bibow, and J.L. Perotti, *Study of the Extended Yard Sale model of wealth distribution on Erdos-Renyi random networks*, arXiv:2505.04032[cond-mat.stat-mech] (2025).

[19] V.E. Zakharov, V.S. L'vov, and G. Falkovich, *Kolmogorov spectra of turbulence*, Springer-Verlag, Berlin (1992).

[20] C. Connaughton, C. Josserand, A. Picozzi, Y. Pomeau, and S. Rica, *Condensation of classical nonlinear waves*, Phys. Rev. Lett. **95**, 263901 (2005).

[21] K. Baudin, A. Fusaro, K. Krupa, J. Garnier, S. Rica, G. Millot, and A. Picozzi, *Classical Rayleigh-Jeans condensation of light waves: observation and thermodynamic characterization*, Phys. Rev. Lett. **125**, 244101 (2020).

[22] E.V. Podivilov, F. Mangini, O.S. Sidelnikov, M. Ferraro, M. Gervaziev, D.S. Kharenko, M. Zitelli, M.P. Fedoruk, S.A Babin, and S. Wabnitz, *Thermalization of orbital angular momentum beams in multimode optical fibers*, Phys. Rev. Lett. **128**, 243901 (2022).

[23] H. Pourbeyram, P. Sidorenko, F.O. Wu, N. Bender, L. Wright, D.N. Christodoulides, and F. Wise, *Direct observations of thermalization to a Rayleigh–Jeans distribution in multimode optical fibres*, Nature Phys. **18**, 685 (2022).

[24] K. Baudi, J. Garnier, A. Fusaro, N. Berti, C. Michel, K. Krupa, G. Millot. and A. Picozzi, *Observation of light thermalization to negative-temperature Rayleigh-Jeans equilibrium states in multimode optical fibers*, Phys. Rev. Lett. **130**, 063801 (2023).

[25] K.M. Frahm and D.L. Shepelyansky, *Nonlinear perturbation of Random Matrix Theory*, Phys. Rev. Lett. **131**, 077201 (2023).

[26] L. Ermann, A.D. Chepelianskii, and D.L.Shepelyansky, *Dynamical thermalization, Rayleigh-Jeans condensate, vortexes and wave collapse in quantum chaos fibers and fluid of light*, arXiv:2506.06534[cond-mat.stat-mech] (2025).

[27] E.P. Wigner, *Random matrices in physics*, SIAM Review **9(1)**, 1 (1967).

[28] M.L. Mehta, *Random matrices*, Elsvier, Amsterdam (2004).

[29] T. Guhr, A. Müller-Groeling and H.A. Weidenmüller, *Random Matrix Theories in quantum physics: common*

concepts, Phys.Rep. **299**, 189 (1998).
[30] A. Aladangady, and A. Forde, *Wealth Inequality and the Racial Wealth Gap*, FEDS Notes Oct 22 (2021); https://www.federalreserve.gov/econres/notes/feds-notes/2021-index.htm, (Accessed 8 June 2025).
[31] E. Chamberlain, *Wealth in Great Britain Wave 4. Chapter 2: Total wealth, Wealth in Great Britain, 2012 to 2014*, 18 Dec 2015; https://www.ons.gov.uk/peoplepopulationandcommunity/personalandhouseholdfinances/incomeandwealth/compendium/wealthingreatbritainwave4/2012to2014/chapter2totalwealthwealthingreatbritain2012to2014 (Accessed 8 June 2025).
[32] F. Cowell, B. Nolan, J.Olivera, and Ph. Van Kerm, *Wealth, Top Incomes and Inequality*, p.175, in *National Wealth*, Eds. K. Hamilton, and C. Herburn, Oxford Univ. Press, Oxford UK (2017),
[33] Holdings SPDR S&P500 ETF Trust of June 16 (2025); https://www.ssga.com/us/en/intermediary/etfs/spdr-sp-500-etf-trust-spy
[34] London stock exchange data of capitalization of companies, December 31 (2024), https://www.londonstockexchange.com/reports?trkcode=lsehomstats&tab=issuers (Accessed 19 June 2025).
[35] Hong Kong stock exchange data of capitalization of companies, June 19 (2025), https://www.hkex.com.hk/Market-Data/Securities-Prices/Equities?sc_lang=en (Accessed 19 June 2025).

Supplementary Material for

Wealth Thermalization Hypothesis

by K. M. Frahm and D. L. Shepelyansky
Laboratoire de Physique Théorique, Université de Toulouse, CNRS, UPS, 31062 Toulouse, France

Submitted June 19, 2025 with additional figures, explanations and analytical formula.

I. GENERAL FEATURES OF THE THERMALIZATION IN THE RJS MODEL

Here we remind a bit more details about thermalization of the RJS model (see also Refs. [25,26] for more details). Let us assume that we have N linear classical oscillators with individual energies E_m, $m = 0, \ldots, N-1$ which are coupled by some small non-linear perturbation (see Ref. [25] for an example) such that there are two conserved quantities being the global (squared) amplitude and total energy:

$$1 = \sum_{m=0}^{N-1} \rho_m \quad , \quad E = \sum_{m=0}^{N-1} E_m \rho_m \tag{S.1}$$

where ρ_m is the time averaged squared amplitude and occupation probability of each oscillator. If the non-linear terms are sufficiently strong or if there is some weak coupling to an external system (which respects both constraints (S.1)) one can assume that the system thermalizes. Applying the framework of the grand canonical ensemble one introduces two parameters: temperature T and chemical potential μ to satisfy both constraints (S.1) in average and it can be shown (see e.g. Ref. [25]) that

$$\rho_m = \frac{T}{E_m - \mu} \quad , \quad T = \frac{E-\mu}{N} \tag{S.2}$$

where the expression for the temperature T is obtained from $\sum_m (E_m - \mu)\rho_m = (E - \mu)$ which follows directly from (S.1). The chemical potential is determined (using standard numerical techniques) by solving the implicit equation:

$$1 = \frac{E-\mu}{N} \sum_{m=0}^{N-1} \frac{1}{E_m - \mu} \tag{S.3}$$

which allows for one physical solution of μ outside the energy interval $[E_{\min}, E_{\max}]$ with either $\mu < E_{\min}$ ($T > 0$) or $\mu > E_{\max}$ ($T < 0$) (depending on the value of E we have either $T < 0$ or $T > 0$) such that $\rho_m > 0$. The data presented in this work were obtained by this procedure for different model spectra and certain values of $N =$

10000 (or $N = 1000$ for the RMT model). Concerning the RJS model we have also considered the cases $N = 100$, $N = 1000$ and verified that the obtained Lorenz curves are very close (in graphical precision).

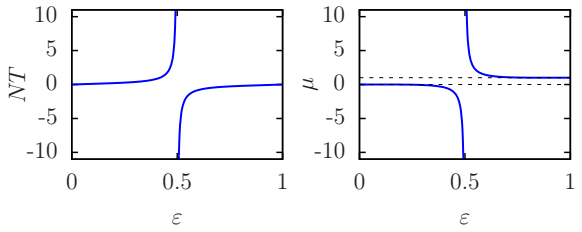

FIG. S1: The left (right) panel shows the (rescaled) temperature NT (the chemical potential μ) versus the rescaled energy $\varepsilon = E/B$ for the RJS model $E_m = m/N$, $N = 10000$. The dashed black lines in the right panel correspond to the values of $E_0 = 0$ and $B \approx 1$ showing that either $\mu < E_0$ (for $T > 0$) or $\mu > B$ (for $T < 0$).

As illustration Fig. S1 shows for the RJS model with $E_m = m/N$, $m = 0, 1, \ldots, N-1$, $N = 10000$ both T and μ as a function of $\varepsilon = E/B$ (here $B = E_{\max} - E_{\min} \approx 1$). Note that the left panel shows the rescaled temperature NT since typical numerical values of T are $\sim 1/N$ due to the finite value of B in our particular model. (We note that the construction of the Lorenz curve is independent of a global scaling factor one could apply to the energy levels.) The figure illustrates that $-\mu \to 0$ ($\mu \to -\infty$) for $\varepsilon \to 0$ ($\varepsilon \to 1/2$).

Using (S.3) one can show that $-\mu \approx E/(N-1) \ll E$ for very small energies $0 < E \ll 1/N$ and in this particular case we have $\rho_0 \approx 1$ (strong condensation) and other $\rho_m \sim E/(NE_m) \ll 1/N$ (for $m > 0$). With increasing values of E (or ε) the values of "$-\mu$" increase and more probability is shifted to the other ρ_m values for $m > 0$. At $\varepsilon \approx 1/2$ we have very large values of "$-\mu$" (and of T) such that all $\rho_m \approx 1/N$ are uniformly constant. Further increase of ε enters the regime of negative temperatures (with $\mu > E_{\max}$) with possible condensation at the last oscillator with $\rho_{N-1} \gg 1/N$ (in this work we do not insist on the regime of $T < 0$). These features are visible in both figures Figs. S2 and S3 showing ρ_m versus E_m/B for different values of ε (as color plot or curves in log-scale). The effect of condensation for small ε with a finite probability $\rho_0 \gg 1/N$ is clearly visible in both figures and qualitatively one could even say that it extends even up to $\varepsilon = 0.2$ with $\rho_0 = 0.002495$ still being larger than $1/N$. However, here also some other values of ρ_m with small m are significantly larger than $1/N$ (as can be seen in S3 for the first 5% of modes with $\rho_m \geq 3/N$). Also the coarse grained average value at the first 5% of modes at $\varepsilon = 0.2$ is roughly 0.35 times the maximal coarse grained value at $\varepsilon \approx 0$ (according to Fig. S2). This effect corresponds to (modest) condensation on several modes or a given small mode interval.

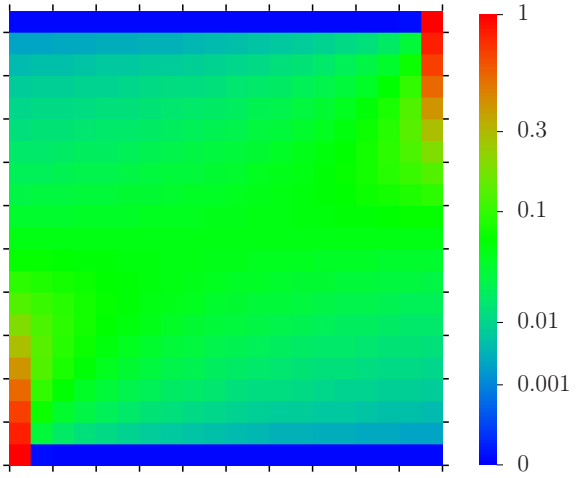

FIG. S2: Color plot of the coarse grained thermalized occupation probabilities $\rho_m = T/(E_m - \mu) = (E-\mu)/[N(E_m - \mu)]$ for the RJS model. The x-axis corresponds to the fraction $E_m/B \in [0, 1]$ (left to right) and the y-axis to the rescaled energy ε (top to bottom for increasing values). The tics indicate integer multiples of 0.1 for both quantities. The color values shown in the color bar correspond to the value of ρ_m averaged over intervals of size 1/20 (for E_m/B on the x-axis) and computed for 21 values $\varepsilon = i/20$, $i = 0, 1, \ldots, 20$ (for the y-axis; the minimal value $\varepsilon = 0$ has been slightly enhanced and the maximal value $\varepsilon = 1$ has been slightly reduced to have a stable computation of the thermalized μ-value). To increase visibility of small values a non-linear color bar scale has been chosen (e.g. green color corresponds to 1/16).

When constructing the Lorenz curve we have $w = 0$ for $h < \rho_0$ and in the presence of (strong) condensation there is a finite interval of households with no wealth at all. Even for modest condensation over several modes the wealth value is initially very low. This can also be seen in Fig. 1 where $w(h \leq 0.1) \approx 0$ for $\varepsilon = 0.2$ showing the effect of modest condensation.

Below, we will present a continuous version of the RJS model with the exact limit $N \to \infty$ and some analytic formulas for the key quantities.

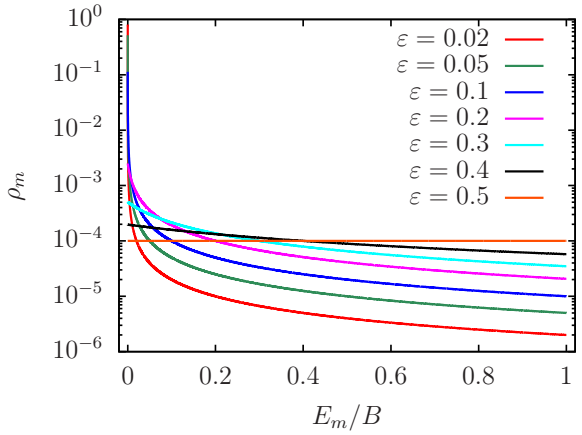

FIG. S3: Dependence of the thermalized occupation probabilities $\rho_m = T/(E_m - \mu) = (E - \mu)/[N(E_m - \mu)]$ on E_m/B for the RJS model $E_m = m/N$, $N = 10000$ and the same values of $\varepsilon = E/B$ used in Figure 1 of the main part.

II. ADDITIONAL DATA

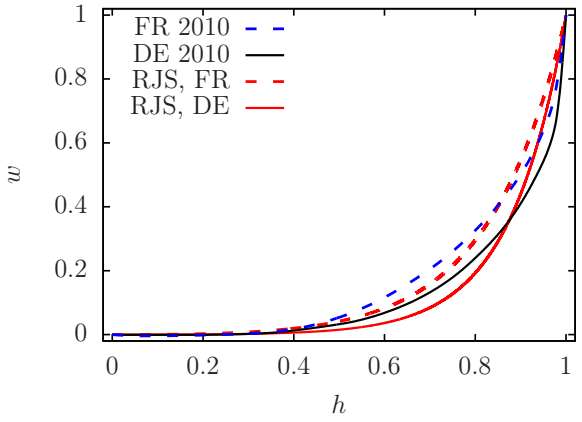

FIG. S4: Comparison of the Lorenz curves for DE 2010 (black) and FR 2010 (blue dashed) with those of the RJS model (red curves; $N = 10000$). The data of DE and FR were extracted from Ref. [32]. As in Fig. 3 the Gini coefficients $G = 0.758$ (DE) and $G = 0.679$ (FR) were used to determine the ε values of the RJS model as $\varepsilon = 0.1220$ (DE) and $\varepsilon = 0.1659$ (FR) to match the Gini coefficients of the reference data.

In this section, we present additional data. First Fig. S4 shows the Lorenz curves from Germany and France and the corresponding curves of RJS model (with matching Gini coefficients). These data were extracted from Ref. [32] with best possible precision and correspond to the period of 2010. The agreement with the RJS is comparable (not perfect but still rather close) as with the cases of US and World in Fig. 3. The Gini coefficients of Germany ($G = 0.758$) and France ($G = 0.679$) are both intermediate between UK ($G \approx 0.62$) and US/World ($G \approx 0.85/0.84$).

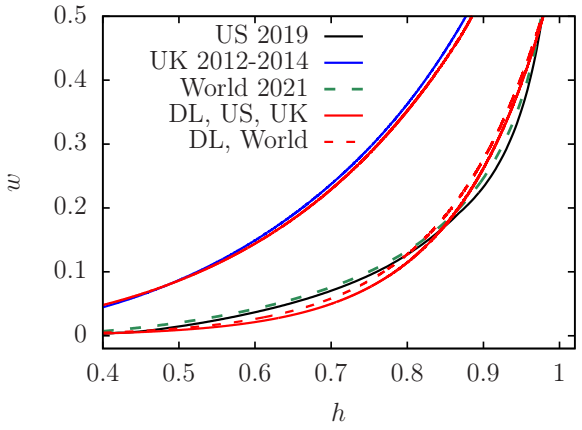

FIG. S5: As panel (b) of Fig. 4 but with a zoomed representation for $h \in [0.4, 1]$ and $w \in [0, 0.5]$ to increase the visibility between the close curves for US 2019 and World 2021.

The next Fig. S5 shows a zoomed representation of panel (b) of Fig. 4 for $h \in [0.4, 1]$ and $w \in [0, 0.5]$ to increase the visibility between the close curves for US 2019 and World 2021 and to also to enhance the small differences with respect to the DL model (red lines).

Furthermore, Fig. S6 presents results for the EQI model with $E_0 > 0$, $E_m = E_0 + m/N$ and $\varepsilon = (E - E_0)/(E_{N-1} - E_0) \approx E - E_0$. In this case, the finite value $E_0 > 0$ induces an initial finite slope $E_0/E = E_0/(E_0+\varepsilon)$ in the Lorenz curve. We have verified that for the four cases shown in Fig. S6 this formula indeed represents the initial slope (see figure caption for the values). In this model, even the poorest households own a significant fraction of the wealth which is given by this slope. Here the range of possible Gini coefficients is quite limited with maximum values of $G_{\max} \approx 0.1$ or 0.4 for $E_0 = 1$ or $E_0 = 0.1$ respectively. Due this reason it is not possible to match the data of US, UK, World etc. (with much larger Gini coefficients) to this model (for the cases shown in Figs. 6 and S6).

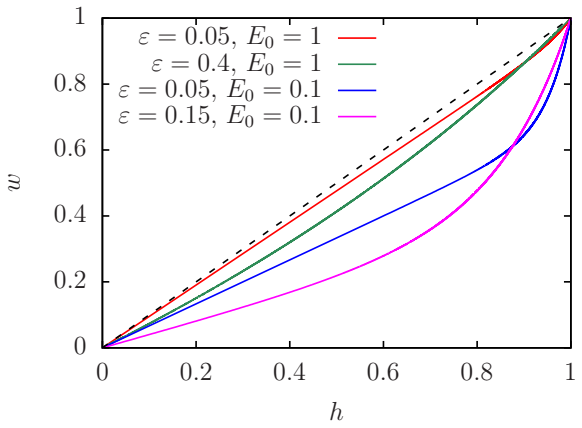

FIG. S6: Lorenz curves of the thermalized EQI model ($N = 10000$) with the two offset values $E_0 = 0.1$ and $E_0 = 1$ and for each case for two values of the rescaled energy $\varepsilon = (E - E_0)/(E_{N-1} - E_0)$. Note that for $E_0 = 1 \Rightarrow E_{N-1} \approx 2E_0$ and for $E_0 = 0.1 \Rightarrow E_{N-1} \approx 11E_0$. The dashed line corresponds to the line of perfect equipartition $w = h$. The Gini coefficients G for all curves are $G = 0.4239$, 0.3000, 0.1162, 0.04286 (bottom to top). These curves show a finite initial slope with value $E_0/(\varepsilon + E_0) = 0.4$, 0.6667, 0.7143, 0.9524 (bottom to top).

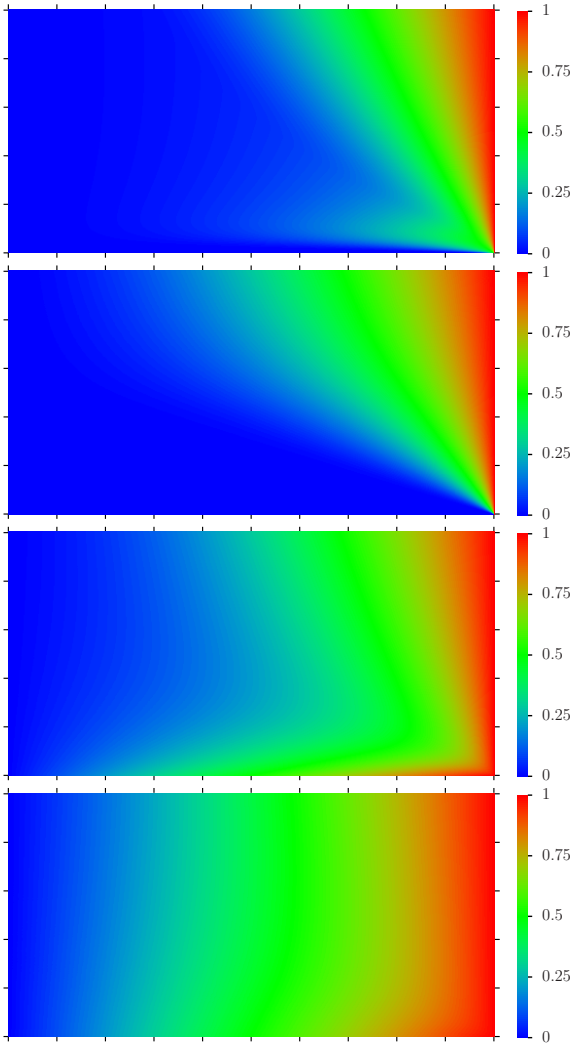

FIG. S7: Color plot of Lorenz curves for different models in the same style of Figure 2. The panels from top to bottom correspond to the DL model with parameter $a = 16$ (1st row), to the shifted RMT semi-circle spectrum (2nd row), to the EQI model with given offset $E_0 = 0.1$ (3rd row) and $E_0 = 1$ (4th row). For the EQI model the rescaled energy $\varepsilon \in [0, 0.5]$ for the vertical axis is given by $\varepsilon = (E - E_0)/(E_{N-1} - E_0)$ (same expression for the other models but with $E_0 = 0$). All cases correspond to $N = 10000$ levels except for RMT with $N = 1000$.

Finally, Fig. S7 shows several color plots in the same style as Fig. 2, i.e. the color value (visible in the color bar) shows w of the Lorenz curve as a function of h (x-axis) and ε (y-axis). The 2nd panel for the RMT model is rather similar to Fig. 2 for the RJS model, with a

slight tendency for smaller G values for $\varepsilon > 0.2$ (at given ε, see also Fig. 5). The first panel for the DL model with $a = 16$ ha a stronger condensation effect (i.e. more poor or poorer households) at $\varepsilon \approx 0.08$ as compared to $\varepsilon \approx 0.03$. Both bottom panels correspond to the EQI model with $E_0 > 0$ (here $\varepsilon = (E - E_0)/(E_{N-1} - E_0)$) with reduced Gini coefficients and where poor people own a significant fraction of the wealth, even at small values of ε.

III. ANALYTICAL RESULTS FOR RJS MODEL

For the RJS model with finite ε it is possible to obtain explicit formulas in the limit $N \to \infty$ by replacing the sums over m with integrals over an energy variable $\tilde{E} = m/N \in [0, 1]$. In the following, we also use $\varepsilon = E$ (since $E_0 = 0$ and $B = (N-1)/N \to 1$ for $N \to \infty$). In the limit $N \to \infty$ the implicit equation (S.3) becomes:

$$1 = (\varepsilon - \mu) \int_0^1 \frac{1}{\tilde{E} - \mu}\, d\tilde{E} = (\varepsilon - \mu) \ln\left(\frac{1-\mu}{-\mu}\right) \quad \text{(S.4)}$$

which can be rewritten in the following form:

$$\mu = -(1-\mu) e^{-1/(\varepsilon-\mu)} \ . \quad \text{(S.5)}$$

Both equations determine μ as a function of $\varepsilon \in]0, 1[$. In the limit of small ε one can simply iterate Eq. (S.5) by inserting $\mu_0 = 0$ in the RHS which gives $\mu_1 = -e^{-1/\varepsilon}$ on the LHS which can be inserted in the RHS to obtain a better value μ_2 etc. This procedure converges nicely for small ε and for other values of ε one can use standard techniques to solve these equations numerically and efficiently. For $\varepsilon \ll 1$, the first approximation $(-\mu) \approx e^{-1/\varepsilon} \ll \varepsilon$ is already very good.

To understand the limit of $|\mu| \gg 1$ it is more useful to consider ε as a function of μ which is determined by (S.4). Expanding the logarithm in (S.4) up to 3rd order in $1/\mu$ one finds that

$$\varepsilon \approx \frac{1}{2}\left(1 + \frac{1}{6\mu}\right) \to \frac{1}{2} \quad \text{(S.6)}$$

for $|\mu| \to \infty$ which is expected from the curve of μ in Fig. S1. The $1/\mu$ correction in (S.6) will be useful below.

As explained in the main part of this work, to compute the Lorenz curve we have to compute a partial sum over ρ_m to obtain the household fraction h and over $(E_m/\varepsilon)\rho_m$ to obtain the wealth variable. Now, we replace these partial sums also by integrals up to some arbitrary value $s \in [0, 1]$ which provides functions $h(s)$ and $w(s)$ allowing to determine the Lorenz curve $w(h)$. These partial integrals are:

$$h(s) = (\varepsilon - \mu) \int_0^s \frac{1}{\tilde{E} - \mu}\, d\tilde{E}$$
$$= (\varepsilon - \mu) \ln\left(\frac{s-\mu}{-\mu}\right) \quad \text{(S.7)}$$
$$\Rightarrow \quad s(h) = (-\mu)\left(e^{h/(\varepsilon-\mu)} - 1\right) \quad \text{(S.8)}$$

and

$$w(s) = \frac{\varepsilon - \mu}{\varepsilon} \int_0^s \frac{\tilde{E}}{\tilde{E} - \mu}\, d\tilde{E}$$
$$= \frac{1}{\varepsilon}\left[(\varepsilon - \mu)s + \mu(\varepsilon - \mu) \ln\left(\frac{s-\mu}{-\mu}\right)\right] . \quad \text{(S.9)}$$

Inserting (S.7) and (S.8) in (S.9) we obtain the following analytical expressions for the Lorenz curve:

$$w(h) = \frac{-\mu}{\varepsilon}\left((\varepsilon - \mu)\left(e^{h/(\varepsilon-\mu)} - 1\right) - h\right) \quad \text{(S.10)}$$
$$= \frac{1-\mu}{\varepsilon}\, e^{-1/(\varepsilon-\mu)}\left((\varepsilon - \mu)\left(e^{h/(\varepsilon-\mu)} - 1\right) - h\right) . \quad \text{(S.11)}$$

Here (S.11) has been obtained by replacing the global factor μ with (S.5) which gives a more convenient expression. Using (S.5), one can verify that (S.10) (and therefore also (S.11)) satisfy the conditions $w(0) = 0$ and $w(1) = 1$.

The expression (S.11) allows to take the limit $\varepsilon \ll 1$ with $\mu \approx -e^{-1/\varepsilon} \ll \varepsilon$ such that for $\varepsilon \ll 1$ we have the simplified Lorenz curve (replacing $\mu = 0$ in (S.11)):

$$w(h) \approx e^{-1/\varepsilon}\left(e^{h/\varepsilon} - 1 - \frac{h}{\varepsilon}\right) \approx e^{(h-1)/\varepsilon} . \quad \text{(S.12)}$$

Here both expression are equivalent approximations for small ε with $e^{-1/\varepsilon} \ll 1$. The first (second) expression does not exactly verify the condition for $w(1)$ (or $w(0)$). The second expression is very simple and numerically quite sufficient for $\varepsilon \leq 0.2$.

We have verified that both expressions (S.10) and (S.11) coincide with the numerical data shown in Fig. 1 up to graphical precision with an error below 10^4 and for all values of ε used in Fig. 1. The approximate formulas (S.12) are valid for $\varepsilon \leq 2$ with an error $\sim 10^{-2}$ for $\varepsilon = 0.2$ (and smaller errors for smaller values of ε). This can be seen in Fig. S8 comparing the data for $\varepsilon = 0.1, 0.2, 0.3$ between the analytic expressions and the

data for $N = 10000$. Even for $\varepsilon = 0.3$ only a modest deviation of the approximate curve is visible while here and in all other cases the more precise expression (S.11) matches the numerical data very closely.

Using the analytical expressions for $w(h)$ one can compute several other quantities. For example it is interesting to consider the 2nd order expansion in h for $|h/(\varepsilon-\mu)| \ll 1$ which gives:

$$w(h) = \frac{(-\mu)}{2\varepsilon(\varepsilon-\mu)}\, h^2 \ . \tag{S.13}$$

We know that the limit $|\mu| \to \infty$ corresponds to $\varepsilon \to 1/2$ and in this case (S.13) is valid for all $h \in [0,1]$. This gives the very simple formula $w = h^2$ (which is also obvious from the fact that $\rho_m = 1/N = \text{const.}$ for $|\mu| \to \infty$ and the way the Lorenz curve is constructed from ρ_m).

It is also possible to compute the Gini coefficient:

$$\begin{aligned} G &= 1 - 2\int_0^1 w(h)\, dh \\ &= 1 + \frac{2\mu}{\varepsilon}\left[(\varepsilon-\mu)^2(e^{1/(\varepsilon-\mu)}-1) - (\varepsilon-\mu) - \frac{1}{2}\right] \qquad \text{(S.14)} \\ &= 1 - \frac{\mu}{\varepsilon} - 2(\varepsilon-\mu)\ . \qquad \text{(S.15)} \end{aligned}$$

Here the second simpler expression (S.15) has been obtained by replacing the exponential term in (S.14) using the implicit equation of μ. The limit $\varepsilon \ll 1$ with $\mu \approx -e^{-1/\varepsilon}$ gives $G \approx 1 - 2\varepsilon$ which matches well the values of G given in the caption of Fig. 1 for $\varepsilon \leq 0.1$ (rather close value for $\varepsilon = 0.2$). The other values are matched exactly by the more precise expression (S.15). Furthermore, inserting the expression (S.6) for large $|\mu|$ in (S.15) one finds (confirms) that $G = 1/3$ for $\varepsilon = 1/2$ (here it is necessary to keep the $1/\mu$ correction in (S.6) to obtain the correct result for G).

Using the analytical expression (S.11) for $w(h)$ it is also straightforward to compute (with simple numerics) the inverse function $h(w)$. Using this and the analytical expression (S.15) for the Gini coefficient, we have also recomputed the curves for $G(\varepsilon)$, $h(2\%)$, $1-h(25\%)$ (both as a function of ε) and verified that the analytical curves coincide with the numerical curves shown in Figs. 5 and 6 (for the RJS model at $N = 10000$) up to graphical precision (typical error $\sim 10^{-4}$).

One might be concerned that the integral approximation is not very good for small μ (close to the singularity of the first term in (S.3)) and some finite but large value of N such as $N = 10000$. This is true but the integral

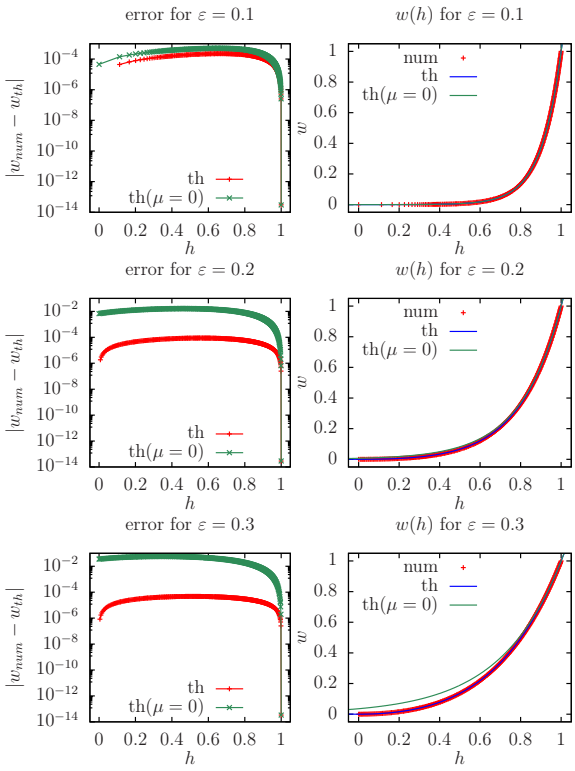

FIG. S8: Comparison of Lorenz curves of wealth fraction w versus household fraction h for the analytical model with the numerical data of the RJS model for finite $N = 10000$ and for three key values of the rescaled energy $\varepsilon = 0.1, 0.2, 0.3$ (top to bottom). Left panels shows the difference between the analytical model and numerical data and right panels show directly the curves w versus h for the numerical data (red lines and plus symbols) and the analytical model. Blue lines/data points correspond to the formula (S.11) valid for all values of ε and using the appropriate value of the chemical potential μ determined by the implicit equation (S.4). Green lines/data points correspond to the (second) approximate formula (S.12) valid for small $\varepsilon \leq 0.2$. The discrete points of data in the top right panel for $\varepsilon = 0.1$ at values close to $w = 0$ indicate finite values for $\rho_0 = 0.1129$, $\rho_0 + \rho_1 = 0.1660$, etc. which are due to RJ condensation.

provides a modified logarithmic singularity which allows also to mimic correctly the condensation effect with correct probabilities. Therefore even though the values of μ are modified for $\varepsilon \ll 1$ (but still $0 < -\mu \ll \varepsilon \ll 1$ for both models !) the resulting probabilities (e.g. integrals or sums of ρ_m over some interval in $\tilde{E} = m/N$) are the same. The values of μ obtained by the continuous analytical model match very well the curve shown in

Fig. S1 but of course this figure does not allow to verify if $\mu \approx -e^{-1/\varepsilon}$ (continuous model) or $\mu \approx -\varepsilon/(N-1)$ (for the finite N model with discrete sums) which are both close to zero in the figure. In any case, we find that the analytical expressions given here (if μ is properly evaluated by its implicit equation (S.4) and if properly evaluated by avoiding numerical instabilities of some formulas in some special cases) match the numerical data with an error that scales with $1/N$.

Without going into details, we mention that we have also considered a more refined version of the continuous model using a finite value of N and keeping the first singular term separate from the integral (which starts at $s = 1/N$ and not $S = 0$). In this case, we obtain a modified implicit equation of μ which results in values of μ closer to the model of finite N but the resulting physical quantities ($w(h)$ curves, Gini coefficients etc.) are (numerically with an error $< 10^{-4}$) the same as both the numerical data and the simple model. The resulting analytical expressions of the refined model are slightly modified (essentially replacing h by $h - \rho_0$ for $h \geq \rho_0$ in the formula of the Lorenz curve and using $w(h) = 0$ for $h < \rho_0$ where ρ_0 may now have a finite value). Note that the initial interval $h \in [0, \rho_0[$ with exactly $w(h) = 0$ for the refined and also the discrete model translates to exponentially small values $w(h) \approx h^2\, e^{-1/\varepsilon}/(2\varepsilon)$ for the simple analytical model (replacing $\mu \approx -e^{-1/\varepsilon}$ in (S.13)).

IV. DATA FOR COMPANIES OF STOCK EXCHANGE AT NEW YORK, LONDON, HONG KONG

We present here the Lorenz curves for the capitalization of companies at stock exchanges of New York, London, Hong Kong. They are obtained respectively from Refs. [33,34,35].

First, we present in Fig. S9 the Lorenz curve for the data of 504 S&P500 companies of the New York Stock Exchange (NYSE) of June 16, 2025 (see Ref. [33]). This Fig. S9 shows the direct comparison of the Lorenz curve of NYSE and the corresponding RJ thermal distribution of the RJS model (at same Gini value). Here, we use the standard value $N = 10000$ for the RJS curve but using a reduced value $N = 504$ (as the number of companies) gives the same RJS curve within graphical precision. The quality of agreement with the RJS model is comparable to the cases of US or World in Fig. 3. We also note the characteristic values: $h = 0.191$ at wealth $w = 0.02$; $w = 0.092$ at $h = 0.5$; the wealth of top 10 percent of h companies is $1 - w(0.9) = 0.602$ and the wealth of top 1 percent of companies is $1 - w(0.99) = 0.267$. Thus we see that there is a small fraction of oligarchic companies that monopolize a big fraction of total wealth. The fraction of poor companies, corresponding to the RJ condensate, is smaller than the fraction of poor housholds in the US or World cases. We attribute this to the fact that these 504 companies of S&P500 represent only about 80 percent of the total capitalization of US companies.

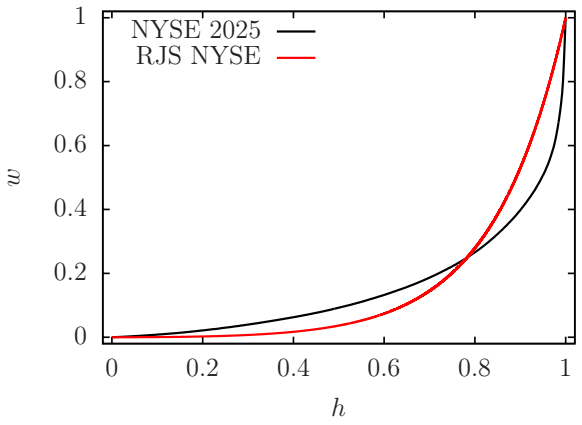

FIG. S9: Comparison of the Lorenz curve for the S&P500 companies of NYSE 2025 (black; data from Ref. [33]) with the corresponding curve for the RJS model (red curve; $N = 10000$) at same Gini coefficient $G = 0.692$ obtained for $\varepsilon = 0.1582$.

Fig. S10, compares the Lorenz curve for the London stock exchange (2024; data from Ref. [34]) with the RJS model. Here, the Gini coefficient $G = 0.9126$ is higher than for the US and World cases and the corresponding value $\varepsilon \approx 0.044$ for the RJS model is quite small. Due to the high value of G the first probability $\rho_0 = 0.6545$ is very high indicating a strong RJ condensation with exactly $w = 0$ for $h \in [0, \rho_0[$ in the RJS model. The chosen value $N = 1637$ is identical to the number of considered companies but the RJS curve for $N = 10000$ is identical on graphical precision (with a slightly modified value for ε).

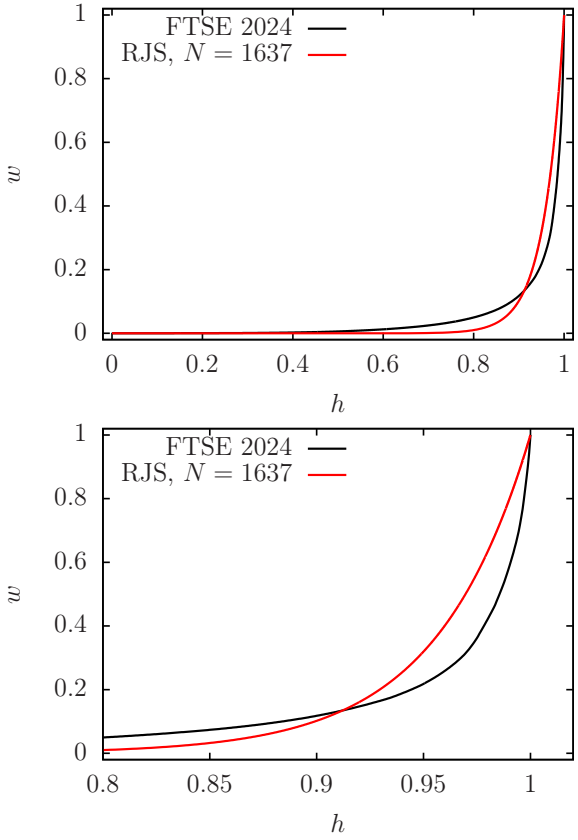

FIG. S10: Comparison of the Lorenz curve for the 1637 companies of the London stock exchange FTSE at 31 December 2024 (black; data from Ref. [34]) with the corresponding curve for the RJS model (red curve; $N = 1637$) at same Gini coefficient $G = 0.9126$ obtained for $\varepsilon = 0.04387$. The top (bottom) panel shows the full range $h \in [0, 1]$ (zoomed range $h \in [0.8, 1]$).

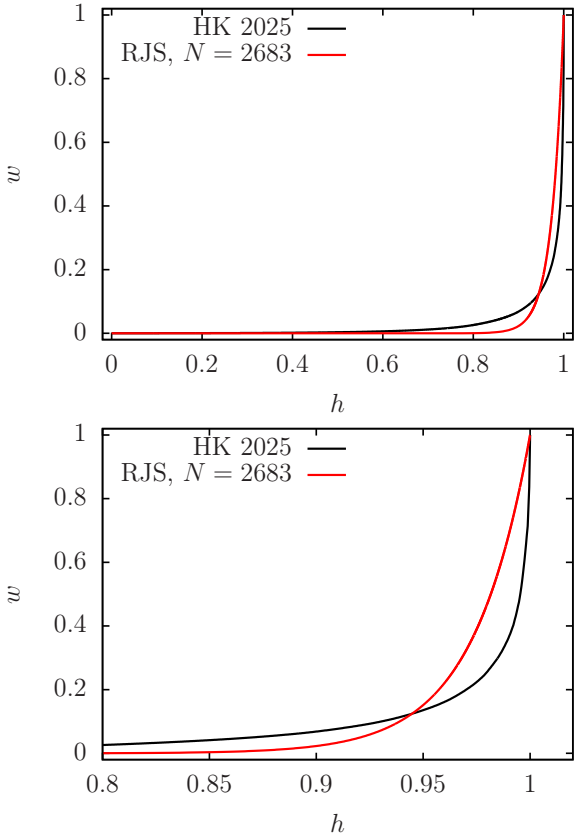

FIG. S11: Comparison of the Lorenz curve for the 2683 companies of the Hong Kong stock exchange at 19 June 2025 (black; data from Ref. [35]) with the corresponding curve for the RJS model (red curve; $N = 2683$) at same Gini coefficient $G = 0.9471$ obtained for $\varepsilon = 0.02651$. The top (bottom) panel shows the full range $h \in [0, 1]$ (zoomed range $h \in [0.8, 1]$).

Fig. S11, compares the Lorenz curve for the Hong Kong stock exchange (2025; data from Ref. [35]) with the RJS model. Here, the Gini coefficient $G = 0.9471$ is even higher than for the London stock exchange and the corresponding value $\varepsilon \approx 0.027$ for the RJS model is even smaller. Due to the very high value of G the first probability $\rho_0 = 0.7768$ is even higher (than ρ_0 for the London stock exchange) indicating a strong RJ condensation with exactly $w = 0$ for the larger interval $h \in [0, \rho_0[$ in the RJS model. The chosen value $N = 2683$ is identical to the number of considered companies but the RJS curve for $N = 10000$ is identical on graphical precision (with a slightly modified value for ε).

Fig. S12, compares the Lorenz curve for the 30 Dow Jones companies (2025; data from Ref. [33]) with the RJS model. Here, the Gini coefficient $G = 0.3096$ is very low and the corresponding value $\varepsilon \approx 0.55$ for the RJS model is very high being in the region for $T < 0$ with large $|T|$. The value of G is even smaller then $G = 1/3$ for the curve $w = h^2$ corresponding to the RJS model with $\varepsilon = 0.5$ and $|T| \to \infty$. The chosen value $N = 30$ is identical to the number of considered companies but despite the modest value of N the RJS curve for $N = 10000$ is identical on graphical precision (with a slightly modified value for ε). We mention, that a comparison with the EQI model for a modest value of E_0 to fit approximately the finite initial slope in the data provides the energy value $\varepsilon \approx 0.48 < 0.5$ corresponding to the regime

of $T > 0$ but still with large $|T|$. We note that this case is very special since these 30 companies are certainly not isolated and they constitute a subset of the 504 companies of S&P500 (which are not perfectly isolated as well).

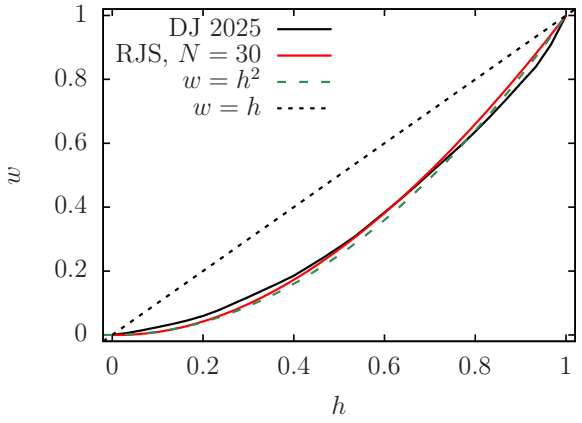

FIG. S12: Comparison of the Lorenz curve for the 30 Dow Jones companies of NYSE 2025 (black; data from the site of Ref. [33] taken at June 18, 2025) with the corresponding curve for the RJS model (red curve; $N = 30$) at same Gini coefficient $G = 0.3096$ obtained for $\varepsilon = 0.5528$. The dashed green (black) line represents the curve for $w = h^2$ ($w = h$) for the RJS model at $\varepsilon = 0.5, T \to \infty$ (perfect equipartition).

For the data of NYSE S&P500 (and Dow Jones companies) the assumption that the system is completely isolated and the total wealth is preserved is somewhat less justified (or not all justified for the Dow Jones case) in comparison to populations of countries or the whole world. We suppose that this fact is the reason for the reduced fraction of poor companies since external fluctuations may increase energies. However, in global the Lorenz curves shown in the section for different stock exchange selections are rather well described by the RJS model but indeed with strongly varying values of ε according to the different values of the Gini coefficient with either $G \approx 1 - 2\varepsilon$ (if $\varepsilon \ll 1$) or $G \approx 1/3$ (if $w \approx h^2$ as in the Dow Jones case).